

Numerical Simulations of Hydrogen Auto-ignition in a Turbulent Co-flow of Heated Air with a Conditional Moment Closure

I. Stanković*,¹, A. Triantafyllidis², E. Mastorakos², C. Lacor³ and B. Merci^{1,4}

¹Ghent University-UGent, Department of Flow, Heat and Combustion Mechanics, Belgium

²Cambridge University, UK

³Vrije Universiteit Brussel, Belgium

⁴Postdoctoral Fellow of the Fund of Scientific Research – Flanders (Belgium) (FWO-Vlaanderen)

Abstract

Our research objective is the performance of Large-Eddy Simulation (LES) with the first order Conditional Moment Closure (CMC) of the test case experimentally studied by Markides and Mastorakos [1]. The experiment concerns auto-ignition of hydrogen, diluted with nitrogen, in a co-flow of heated air. A 19 step, nine species detailed mechanism is used for the reaction. Simulations reveal that the injected hydrogen mixes with co-flowing air and a diffusion flame is established. The configuration is sensitive to inlet boundary conditions, as all major turbulence effects are expected to be dominated by the inflow conditions. Preliminary LES results are presented. Stand-alone chemistry calculations are also presented to illustrate sensitivity on chemistry mechanisms.

Introduction

Auto-ignition is a fundamental problem of practical interest. In many combustion devices it involves interaction between chemistry and turbulence. Further development of the next generation of low NO_x diesel and homogeneous charge compression injection engines and lean premixed prevaporized gas turbines is strongly dependent on capabilities to predict interaction between turbulence and the slow chemistry leading to auto-ignition.

In order to extend understanding of these phenomena, Markides et al [1] performed experiments of the auto-ignition of hydrogen diluted with nitrogen, issued into a co-flow of pre-heated air. In the experiment, the co-flow temperature was varied in order to obtain different auto-ignition regimes (“no-ignition” regime, “random spots” regime, flashback, and lifted flame).

Any method for accurately predicting auto-ignition phenomena by means of numerical simulations has to incorporate turbulence, unsteady chemistry and detailed mechanisms. In combusting flows chemical reaction occurs at scales below the sub-grid dimensions and therefore modeling is required. One of the possible choices for modeling is the Conditional Moment Closure (CMC) [2]. The CMC method is a mixture fraction based approach where the fluctuations of the reacting scalars are considered to be correlated with those of the mixture fraction. Equations are solved for the conditionally averaged reacting scalars, conditioned on mixture fraction, where mixture fraction fully describes the state of mixing of the fluids. The chemical kinetics leading to ignition are complex and detailed chemical mechanisms have to be taken into account. As a consequence, the choice of the chemical mechanism can be of great importance, especially at low temperatures where there is larger uncertainty in the

reaction rate constants. Crucial are intermediates and slow reactions, which increase the pool of reactants. The specific objectives of this paper are: (i) application of the LES/CMC methodology to the test case carried out by Markides and Mastorakos [1]; (ii) influence of the chemistry mechanism by stand-alone chemistry calculations; (iii) to examine influence of inlet boundary conditions.

Experimental Set-up

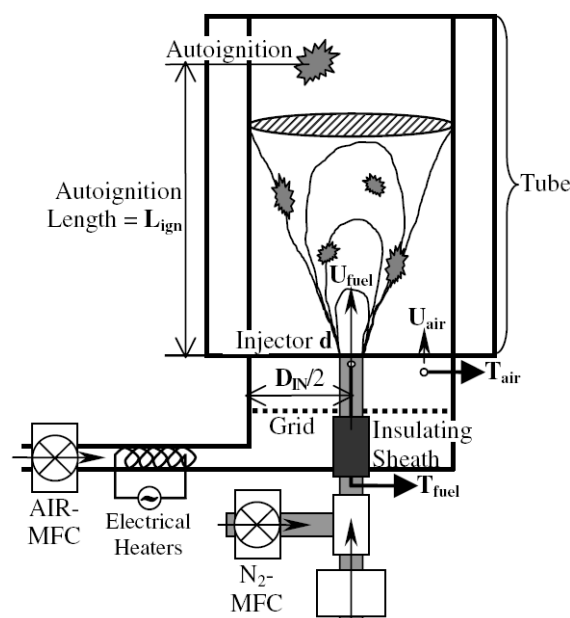


Figure 1 The experimental set-up.

Figure 1 illustrates the set-up [1]. Hydrogen, diluted with nitrogen, is used as a fuel. The fuel is injected into an air co-flow through a 2.25mm internal diameter nozzle at ambient pressure. The burner inner diameter is

* Corresponding author: Ivana.Stankovic@UGent.be
Proceedings of European Combustion Meeting 2009

25mm. Air velocities up to 35m/s, with air temperature up to 1016K, have been achieved. The fuel velocity ranged from 20 to 120m/s, with fuel temperature between 650K and 930K.

Different auto-ignition regimes (no ignition, random spots, flashback and lifted flame) are obtained by varying the temperature of the air and the inlet jet velocity. At the lowest co-flow temperature the “no-ignition” regime was obtained, followed by a “random spot” regime, where auto-ignition kernels appear and are subsequently transported out of the domain. In the “flashback” regime ignition occurs downstream of the nozzle and travels back towards the injector, resulting in a flame. In the observed configuration all major turbulence effects are expected to be dominated by the inflow conditions.

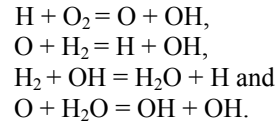
Numerical Set-up

As flow field solver, we use an in-house LES code, developed at VUB [3], with standard Smagorinsky sub-grid scale modeling (with $C_s = 0.1$). In the LES code, the convective fluxes in the momentum equation are discretized with a second order central scheme. For the mixture fraction equation, it is possible to choose between first order upwind or a second order TVD scheme. In this study, the second order TVD scheme has been used. In the CMC code, species and energy equations are solved, using velocity and mixing fields from the flow field solver. Conditional moments are computed at fixed locations and time within the flow field. The CMC code has been developed at Cambridge University [4].

In order to obtain the mean density, required for the flow calculations, the conditionally averaged values, obtained from the CMC calculations, are weighted by the mixture fraction probability density function (PDF) for computation of the unconditional mean values. We use pre-assumed β -PDF shapes. Due to the weaker spatial dependence of the conditional quantities, a coarser spatial grid can be used in the CMC calculations than the LES mesh [4]. This is important because the use of complex chemical mechanisms can be computationally expensive and implies that the size of the system to be integrated can be very large. The system size depends on the number of nodes in mixture fraction space and the number of scalars. The CMC equations are solved using an operator splitting method where a sequential integration of physical-space, diffusion in η -space and the conditional reaction rate is applied. The VODPK solver is used. The solver is based on a linear multistep method using the Backward Differentiation Formula (BDF). It is an implicit solver and can be used both for stiff and non-stiff systems with a large number of ordinary differential equations (ODEs).

In our LES calculations, we use the detailed chemical mechanism for hydrogen of [5]. The mechanism consists of 9 species (H_2 , H, O, O_2 , OH, H_2O , HO_2 , H_2O_2 , and N_2) and 19 reactions. The H_2/O_2 chain reactions play a prominent role in determining the

composition of the radical pool and initiating auto-ignition:



After auto-ignition, the dominant reactions are the formation and consumption of H_2O and species like O, OH and H are formed.

The CFD mesh consists of 96 x 48 x 48 cells, covering a domain of 135mm x 25mm x 25mm. The CMC mesh consists of 16 x 4 x 4 cells. The implementation is parallel, with 4 blocks in the axial direction. As mentioned, the boundary conditions for the simulations (Table 1) are taken from [1]. The stoichiometric mixture fraction ζ_{ST} is 0.184 with the given fuel and oxidizer compositions.

Region	Item	$U_{jet} > U_{air}$
Fuel jet	Velocity, U_{jet} (m/s)	120
	Temperature (K)	691
	Composition	$Y_{H_2} = 0.13$ $Y_{N_2} = 0.87$
Co-flow	Velocity, U_{air} (m/s)	26
	Temperature (K)	960 - 1016
	Composition	$Y_{O_2} = 0.233$ $Y_{N_2} = 0.767$

Table 1 Boundary conditions for the simulation [1].

First studies confirm that it is very important to apply proper turbulence at the inlet boundary of the CFD mesh in order to obtain realistic results (see below). In order to mimic the turbulence generated by the metallic grid of the experimental set-up, a separate LES simulation was performed. In this separate simulation, the air is injected through nine separate square holes (5x5mm), with a blockage factor of 64% (Figure 2). The bulk velocity of the inflow air is chosen such that the outlet velocity corresponds to the inlet velocity as required for the auto-ignition simulations. The jets create the turbulence in their shear layers. The solution domain of the separate simulation is 3 burner diameters (75mm) long. The outlet plane results are used as inlet boundary conditions for the LES/CMC simulation.

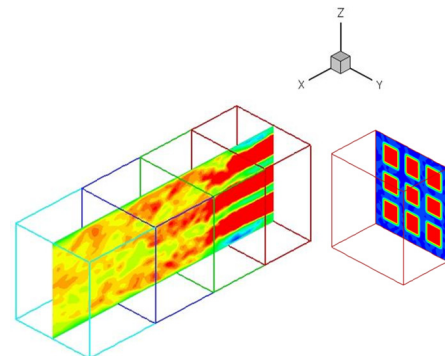


Figure 2 Axial velocity profiles (LES pre-calculation).

The solution strategy is then as follows: first, a developed turbulent mixing field is computed, by deactivating the chemical source term in the CMC equations; then, chemistry is activated and auto-ignition occurs. In the future, the digital filter procedure for generation of the in-flow turbulence [6] will also be applied in order to investigate the sensitivity of the results more completely.

Auto-ignition: Stand Alone Chemistry

A priori calculations are carried out with a stand alone CMC. Conditioning is performed on mixture fraction: $Q(\eta; x, t) \equiv \langle Y(x, t) | \xi(x, t) = \eta \rangle \equiv \langle Y(x, t) | \eta \rangle$, where η denotes the sample space variable for the mixture fraction, ξ . The governing equations for conditional moment closure of species and temperature are:

$$\frac{\partial Q}{\partial t} = \langle N | \eta \rangle \frac{\partial^2 Q}{\partial \eta^2} + \langle W | \eta \rangle \quad (1)$$

$$\frac{\partial Q_T}{\partial T} = \langle N | \eta \rangle \left[\frac{1}{c_{p_n}} \left(\frac{\partial c_{p_n}}{\partial \eta} + \sum_{i=1}^n c_{p_i} \frac{\partial Q_i}{\partial \eta} \right) \frac{\partial Q_T}{\partial \eta} + \frac{\partial^2 Q_T}{\partial \eta^2} \right] - \frac{1}{c_{p_n}} \left\langle \sum_{i=1}^n h_i W_i \right\rangle | \eta \rangle \quad (2)$$

Spatial diffusion and convection are not taken into account, in contrast to what is done in the LES/CMC calculations. The conditional scalar dissipation rate is imposed using the AMC model [7], parameterized on its maximum value at $\eta = 0.5$ (N_{max}):

$$\langle N | \eta \rangle = \frac{G(\eta)}{\int_0^1 G(\eta) \tilde{P}(\eta) d\eta} N_{max} \quad (3)$$

$$G(\eta) = \exp(-2(\text{erf}^{-1}(2\eta - 1))^2) \quad (4)$$

We cover the following range in maximal scalar dissipation rate: $N_{max} = 0.1, 0.5, 1.0, 5.0, 10.0, 20.0, 30.0, 40.0, 50.0, \text{ and } 200.0 \text{ s}^{-1}$. We also cover a range of co-flow temperatures: $T_{cf} = 945, 960, 985, 994, 1003, 1009 \text{ and } 1016 \text{ K}$. The fuel temperature is kept constant: 691K. The simulations are done in order to examine the influence of different chemical mechanisms for hydrogen combustion, for different scalar dissipation rates and co-flow temperatures. We also discuss sensitivity of the results on the discretization in mixture fraction space.

In this study, auto-ignition is defined as the moment when the temperature increases 1% over the nominal co-flow temperature [8]. The criterion is used to determine ignition delay times. For the present configuration, different ignition criteria, found in the literature [9], do not lead to any significant difference in predicted ignition delay times (τ_{ign}) (not shown).

Five different chemical mechanisms are tested:

- Li et al [5],
- Yetter et al [10],
- Mueller et al [11],
- O'Conaire et al [12] and

- Konnov [13].

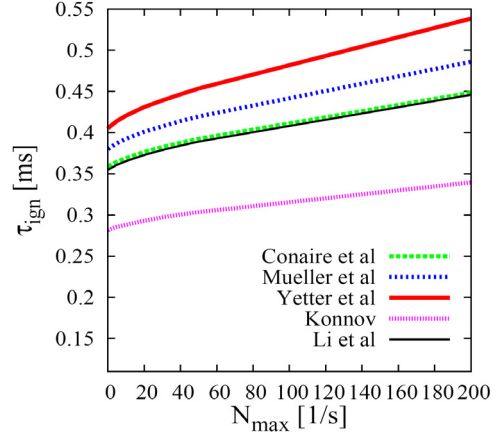


Figure 3 τ_{ign} as a function of N_{max} , $T_{cf} = 1009 \text{ K}$.

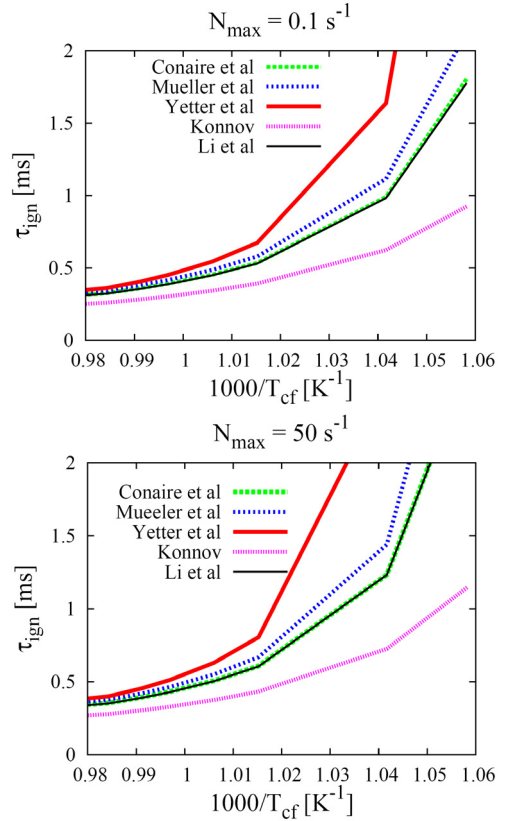


Figure 4 Influence of T_{cf} on the ignition delay time.

The choice of chemistry appears to be critical factor in the simulations. For the entire range of scalar dissipation rates, the Konnov [13] mechanism is the fastest, while the Yetter [10] mechanism is the slowest (Figure 3) for $T_{cf} = 1009 \text{ K}$. Note that the curves do not cross. For higher conditional scalar dissipation rate, auto-ignition is retarded. This is also the case for the other values of T_{cf} . We present results for $T_{cf} = 1009 \text{ K}$ as this is the co-flow temperature in the LES results later. The mechanisms given by Li et al [5] and O'Conaire et al [12] give very similar results. These two mechanisms

also have already been validated for a wide range of experimental conditions. In the full calculation we use the mechanism given by Li et al [5].

The influence of T_{cf} on the auto-ignition delay time is shown in Figure 4. Clearly, τ_{ign} strongly depends on the initial co-flow temperature and decreases with an increase in temperature. The same trend has been demonstrated experimentally: the ignition length increase for lower T_{cf} . With increasing co-flow temperature, differences in τ_{ign} predictions with different mechanisms diminish. The influence of the co-flow temperature is clearly stronger than the impact of the conditional scalar dissipation rate. Figure 4 also reveals that the sharp increase of τ_{ign} occurs only for lower T_{cf} and for the ‘faster’ chemistry mechanisms. The mixture fraction, for which the auto-ignition occurs first, is called ‘most reactive’ mixture fraction (η_{MR}) [14]. Figure 5 presents, for the Li mechanism [5] the

influence of the co-flow temperature on the location of η_{MR} . Results with different resolutions in mixture fraction space are compared. With increase of the co-flow temperature, the ignition delay time becomes shorter and η_{MR} shifts towards richer mixture fractions. This is best visible for lower N_{max} . Since ignition occurs at the lean side, special care should be given to the resolution in mixture fraction space and clustering around η_{MR} . Clearly, clustering of the nodes around η_{MR} is very important. When the nodes are clustered around $\eta_{ST} (= 0.184)$, the location of η_{MR} remains unresolved, as there are not enough nodes in η -space. Figure 5 shows only small difference between results with 51 nodes or 101 nodes (IGRID). This is important, as a reduction in the number of nodes reduces the system of equations to be solved and thus the computational costs.

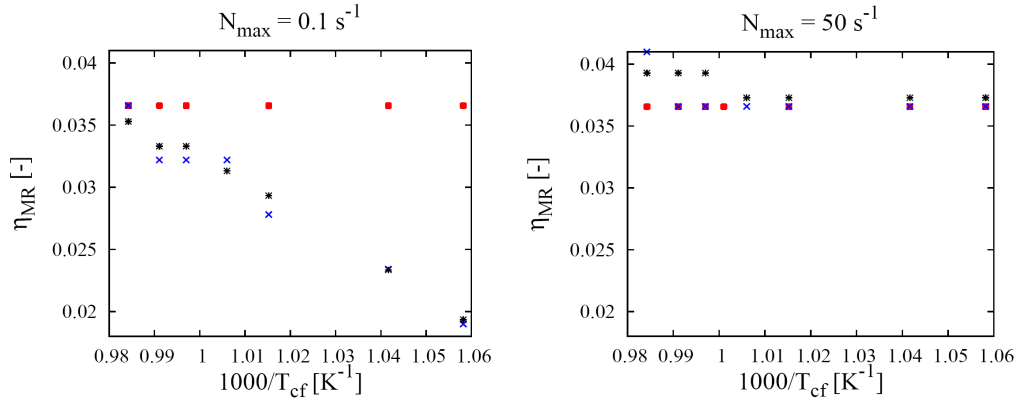


Figure 5 Influence of grid resolution in mixture fraction space: IGRID = 51 with clustering around η_{ST} (squares), IGRID = 51 with clustering around η_{MR} (crosses), IGRID = 101 with clustering around η_{MR} (stars) for two different values of N_{max} .

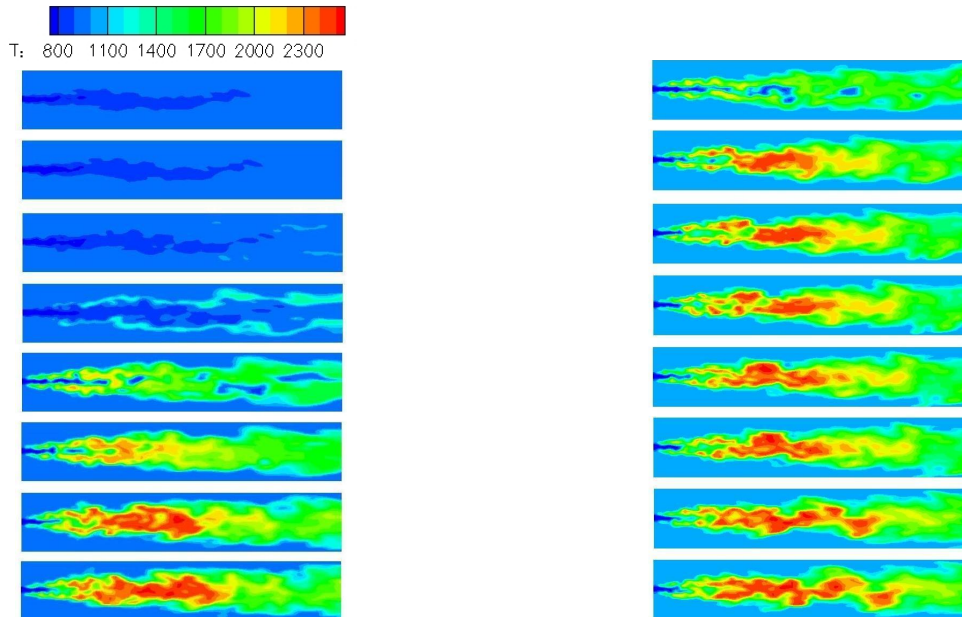


Figure 6 Instantaneous temperature fields in a symmetry plane in physical space for $T_{cf} = 960\text{K}$ (left) and $T_{cf} = 1009\text{K}$ (right) for different times after activation of chemistry in the LES/CMC simulation.

Results: Fully Coupled Calculations

In the present study, only the co-flow temperature is varied, while maintaining the velocity of the fuel and co-flow stream constant. Figure 6 presents instantaneous snapshots of temperature fields at different times after activation of chemistry in a symmetry plane. The delay in ignition with decrease of the co-flow temperature, as demonstrated with a stand alone CMC results, is confirmed.

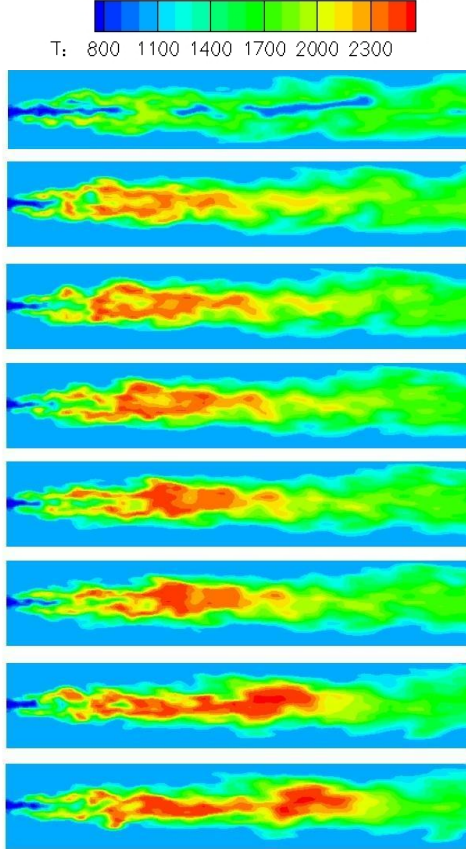


Figure 7 Instantaneous temperature fields in physical space obtained using dynamic Smagorinsky model ($T_{cf} = 1009\text{K}$).

Figure 7 shows the same results, but with a dynamic Smagorinsky sub-grid viscosity model. The temperatures during the initial stages are slightly lower than the ones obtained with a standard Smagorinsky model. Mixing is indeed slightly less intense: the dynamically predicted Smagorinsky coefficient, C_s , varies between 0.075 and 0.1 in the domain. As the difference with $C_s = 0.1$, used in the constant Smagorinsky model, is not big, there is generally no significant difference between the results.

In Figure 8, we illustrate the influence of the inlet boundary conditions. Here, we examine unconditional instantaneous temperature fields in physical space. The upper results are with the previously generated data set. In fact, this corresponds to Figure 6 (right). For the simulation results on the bottom of Figure 8, white noise is imposed, keeping all other settings identical. As is well known, such artificial turbulence disappears very

quickly, so that this almost resembles laminar inflow conditions. Clearly, (proper) turbulence enhances mixing, leading to higher temperatures closer to the nozzle and shorter flames.

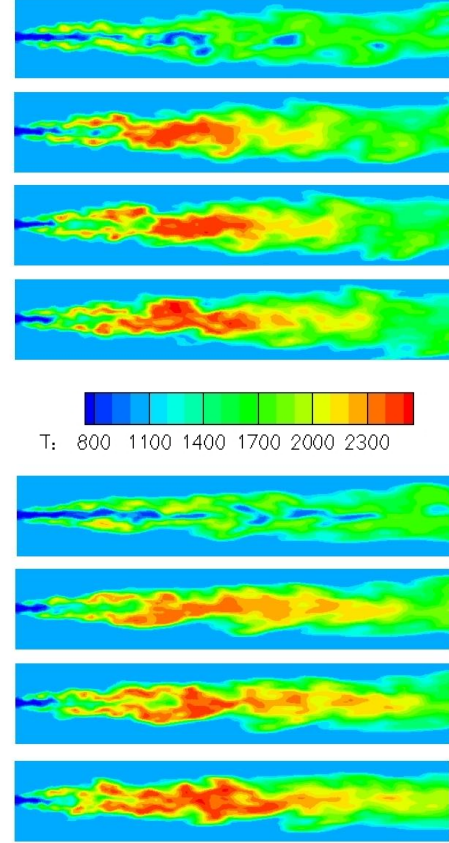


Figure 8 Instantaneous temperature fields in a symmetry plane in physical space ($T_{cf} = 1009\text{K}$). Upper: turbulent co-flow. Lower: white noise as turbulence at the inlet.

We now discuss the evolution of the location of high temperature regions in physical space (Figure 9). As mentioned, the most reactive mixture fraction corresponds to the mixture fractions with a minimum auto-ignition time and low scalar dissipation rate. It is characterized by the maximum gradient of temperature, which suggests that an auto-ignition definition based on a temperature threshold can be used. An a priori analysis, reveals that the location of the most reactive mixture fraction depends on the chemistry (not shown), as well as on the initial conditions in temperature and scalar dissipation rate (see above). Figure 9a shows inert flow (before ignition). Figure 9b indicates that the first chemical reactions clearly occur at the lean side. The temperature increase is visible at the side of the hot co-flow, while the fuel in the center is still cold. As the chemical reaction becomes more important, the maximum temperature increases and shifts towards higher mixture fractions (Figure 9c and d). When chemistry finally takes place for all mixture fractions, the maximum temperature is reached around the stoichiometric mixture fraction (Figure 9e).

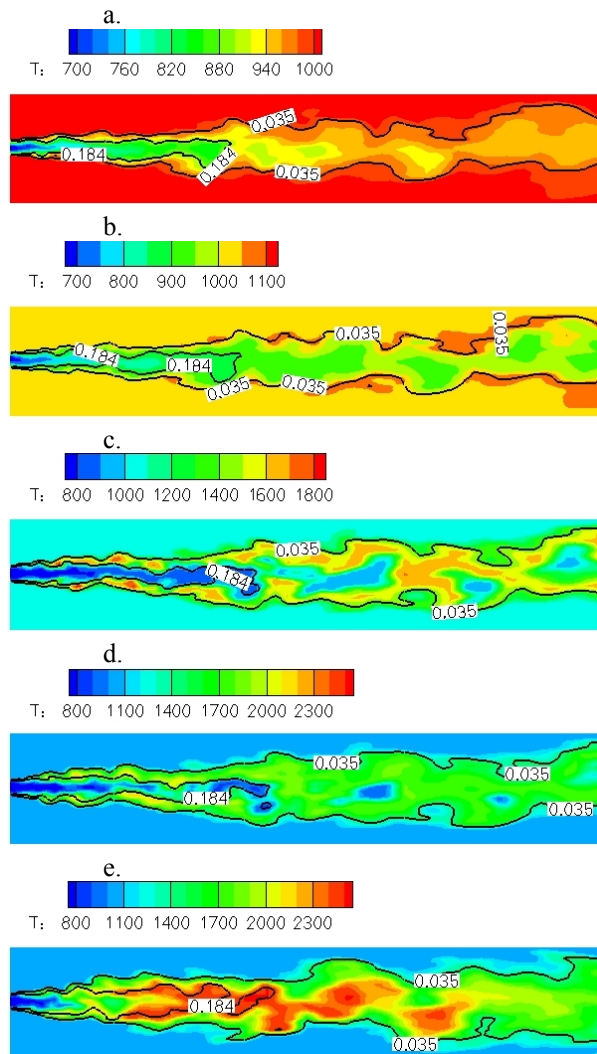


Figure 9 Instantaneous planar temperature fields with the most reactive mixture fraction (outer line) and stoichiometric mixture fraction isolines (inner lines), $T_{cf} = 1009\text{K}$.

Conclusions

LES results, with first order CMC, have been presented for hydrogen auto-ignition in a turbulent co-flow of heated air, using detailed chemistry. The analysis of instantaneous temperature fields agrees with

a priori findings on auto-ignition. The first chemical reactions appear for the most reactive mixture fraction, at the lean side. The co-flow temperature has a strong influence on the auto-ignition. Increasing the co-flow temperature from 960K to 1009K, changes the behaviour of the flame. At higher air temperature ignition occurs more rapidly.

Acknowledgements

This work has been funded by FWO project G.0079.07.

References

- [1] C.N. Markides, E. Mastorakos, Proc. Comb. Inst. 30 (2005) 883-891.
- [2] A. Y. Klimenko, R.W. Bilger, Prog. Energy Combust. Sci. 25 (1999) 595-687.
- [3] T. Broeckhoven, PhD Thesis, VUB, http://mech.vub.ac.be/thermodynamics/phd/list_lacor.htm (2007).
- [4] Y. M. Wright, G. De Paola, K. Boulouchos and Mastorakos, Combust. Flame, 143 (2005) 402-419.
- [5] J. Li, Z. Zhao, A. Kazakov and F. L. Dryer, Int. J. Chem. Kinet. 36 (2004) 566-575.
- [6] M. Klein, A. Sadiki, J. Janicka, J. Comput. Phys. 10 (2003) 1246-8.
- [7] E.E. O'Brien, T. Jing, Phys. Fluids A, 3 (1991) 3121-3123.
- [8] W.P. Jones, S. Navarro-Martinez, O. Rohl, Proc. of Comb. Inst. 31: (2007) 1765-1771.
- [9] R.R. Cao, S.B. Pope, A.R. Masri, Combust. Flame, 142 (2005) 438-453.
- [10] R. A. Yetter, F. L. Dryer, H. Rabitz, Combust. Sci. Technol. 79 (1991) 97-128.
- [11] M.A. Mueller, T.J. Kim, R.A. Yetter, F. L. Dryer, Int. J. Chem. Kinet. 31 (1999) 113-125.
- [12] M. O' Conaire, H. J. Curran, J. M. Simmie, W. J. Pitz, C. K. Westbrook, Int. J. Chem. Kinet. 36 (2004) 603-622.
- [13] A. Konnov, Comb. Flame, 152 (2008) 507-528.
- [14] E. Mastorakos, T.A. Baritaud, and T.J. Poinot, Comb. Flame, 109 (1997a) 198-223.